Available online at www.sciencedirect.com

SCIENCE DIRECT

Surface & Coatings Technology 185 (2004) 321–328

SURFACE & COATINGS TECHNOLOGY

www.elsevier.com/locate/surfcoat

# Improving the corrosion resistance of NdFeB magnets: an electrochemical and surface analytical study

A. Saliba-Silva[a], R.N. Faria[a], M.A. Baker[b], I. Costa[a,*]

[a] *IPEN/CNEN-SP, Av. Prof. Lineu Prestes, Sao Paulo, SPCEP 05508-000, Brazil*
[b] *School of Engineering, University of Surrey, Guildford, Surrey, GU2 7XH, UK*

Received 8 July 2003; accepted in revised form 19 December 2003
Available online 16 March 2004

**Abstract**

This study reports the results of work carried out to improve the corrosion resistance of NdFeB magnets by a direct phosphate treatment of the NdFeB magnet surface. The growth of a phosphate film on a NdFeB based magnet in a solution of 0.15M $NaH_2PO_4$ acidified to pH 3.8, was followed by electrochemical impedance spectroscopy (EIS) and open circuit potential variation as a function of time. After removal from the phosphating solution, the magnet surface was analysed by Auger electron spectroscopy (AES) and energy dispersive X-ray analysis (EDX). Phosphate formation on the surface was confirmed and a significant variation in the Fe/Nd ratio in the phosphate between the Fe and Nd rich phases of the magnet was found. The corrosion resistance of the phosphated magnets was evaluated in a normal enclosed atmospheric environment and in $Na_2SO_4$ solution and synthetic saliva by EIS measurements. The corrosion resistance was found to be substantially improved by the presence of a phosphate layer.


*Keywords:* Corrosion; Impedance spectroscopy; Auger electron spectroscopy (AES); Chemical conversion

## 1. Introduction

NdFeB based magnets were developed in the beginning of the 1980s. They have a maximum energy product between 36 MGOe and 50 MGOe, and are progressively replacing Sm–Co magnets (maximum energy product 33 MGOe). Despite their excellent magnetic properties, NdFeB magnets are unstable at moderate to high temperatures and are highly susceptible to corrosion in environments of high humidity. The literature has associated the low corrosion resistance of these magnets to their complex microstructure [1–9]. The main phases of NdFeB magnets are the magnetic phase ($\phi$), that is Fe rich, and a Nd rich phase. The different electrochemical potentials arising from a multiphase composition leads to galvanic corrosion in the presence of an electrolyte [6,9–12].

NdFeB magnets are usually produced by powder metallurgy (P/M). The Nd rich phase is one of the most active phases present in the P/M NdFeB magnets. Preferential attack of this phase gives rise to intergranular corrosion [9], leading to detachment of $\phi$ grains, and eventually disintegration of the material [8,9]. This causes deterioration of the magnetic properties and can affect the performance of other components in the neighborhood, due to loose corrosion products on the surface [10–12].

Much of the effort to improve the corrosion resistance of NdFeB magnets has concentrated on the use of coatings to protect the magnet [5,12–14]. Attempts have also been made to increase the corrosion resistance of NdFeB based magnets by the addition of alloying elements [2,3,6,8,15]. However, alloying often deteriorates the magnetic properties and despite the improvements made by the addition of alloying elements, protective coatings are still needed for practical applications. In addition to corrosion protection, coatings on NdFeB magnets bind magnetic particles which otherwise would be loose. This is particularly important in applications such as computer components, where the surface must be clean and free of such debris [12].

* Corresponding author. Tel.: +55-11-3816 9356; fax: +55-11-38169370.
*E-mail address:* icosta@ipen.br (I. Costa).

0257-8972/$ - see front matter © 2004 Elsevier B.V. All rights reserved.
doi:10.1016/j.surfcoat.2003.12.015

Table 1
Chemical composition of NdFeB magnets (at.%)

| Fe | Nd | B | Dy | Al | Co | Si | Cu | Nb |
|---|---|---|---|---|---|---|---|---|
| 67.9 | 12.3 | 5.8 | 0.8 | 8.1 | 1.4 | 3.1 | 0.2 | 0.4 |

One method of corrosion protection overlooked in the literature is the use of conversion coatings. These are often used as pretreatments before coating application, increasing the corrosion resistance in defective regions of the coating. One of the most effective conversion coating processes is chromatizing, but the toxicity of this process has led to concerns and curbs on its use. Phosphating on the other hand, is an environment friendly surface treatment. The corrosion behavior of phosphate coated NdFeB magnets has recently been investigated and promising results have been obtained [16–19]. Furthermore, it is well known that phosphating also promotes adhesion of the substrate material if further protective layers are to be applied.

The object of this work is to study the formation of phosphate coatings on sintered NdFeB magnets and to evaluate the corrosion resistance of phosphated NdFeB magnets in mildly corrosive environments. The growth of the surface layer on a commercial NdFeB obtained by immersion in a solution of $NaH_2PO_4$ was investigated as a function of time by means of electrochemical impedance spectroscopy (EIS) and open circuit potential (OCP) measurements. Auger electron spectroscopy (AES) and energy dispersive X-ray analysis (EDX) have been employed to study the chemical composition of the phosphate on the Fe rich and Nd rich phases of the magnet after treatment.

## 2. Experimental procedure

### 2.1. Material

The material used for phosphating was a NdFeB commercial magnet produced by a powder metallurgical route and supplied by CRUCIBLE Co. (known as Crumax). The chemical composition of the magnet is given in Table 1.

The hydrostatic density of the NdFeB magnets used in this study is ($7.58\pm$g cm$^{-3}$) whereas the theoretical density of NdFeB is 7.600 g cm$^{-3}$.

### 2.2. Specimen preparation

The NdFeB specimens were cold resin mounted after an electrical contact (with copper wire) was made to one of their surfaces. A surface area of 1.25 cm$^2$ was exposed to the phosphating solution and subsequently used for corrosion testing. The surface of the electrode was prepared by sequential grinding with silicon carbide paper from grit #120 to #2000, followed by rinsing with deionized water and drying under a hot air stream.

### 2.3. Electrochemical tests

Polished NdFeB samples were immersed in a naturally aerated 0.15 M $NaH_2PO_4$ solution with the pH adjusted to 3.8, at ($22\pm1$)°C. A three electrode cell arrangement was used for the electrochemical measurements, with a graphite rod and a saturated calomel electrode (SCE) as counter and reference electrodes, respectively. EIS measurements were performed with a 1255 Solartron frequency response analyzer coupled to an EG&G 273A Potentiostat running in the potentiostatic mode at the open circuit potential, $E_{ocp}$. The amplitude of the perturbation signal was 10 mV, and the frequency range studied from $10^5$ to $10^{-2}$ Hz with 7 points per decade.

### 2.4. Corrosion tests

Magnets were immersed in the pH adjusted 0.15 M $NaH_2PO_4$ solution (as described above) for periods of 4 and 18 h. After phosphating the samples were dried and re-immersed in 0.01 mol l$^{-1}$ $Na_2SO_4$ and synthetic saliva solution to evaluate their corrosion resistance to mildly aggressive media. Specimens of phosphated and unphosphated magnets were also stored in the laboratory to assess their corrosion performance in a normal enclosed atmospheric environment.

### 2.5. Auger and EDX analysis

Chemical characterization by AES and EDX of phosphate films formed by immersion of NdFeB magnet in 0.15 M $NaH_2PO_4$ solution for 24 h was carried out using a VG Microlab mk II onto which an EDX detector had been mounted. AES point spectra were acquired using an electron beam operating at 15 keV and specimen current of 10–15 nA. The spectra were acquired at a constant retard ratio (CRR) of 4, step of 1 eV, for general wide scans and CRR 10, step 0.3 eV, for the phosphorous KLL region analysis.

## 3. Results and discussion

Fig. 1 shows an SEM image of an untreated NdFeB magnet.

The white regions correspond to the Nd rich phases, the grain size is <5 μm, and the gray surface is the main magnetic phase ($\phi$ phase). The darker areas are cavities, mainly caused by removal of particles during mechanical polishing, but also pores resulting from the fabrication process (powder metallurgy).

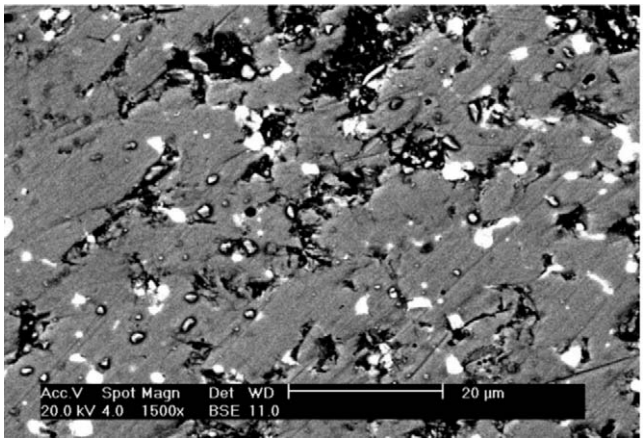


Fig. 1. SEM image of untreated NdFeB magnet.

Fig. 2 shows a typical $E_{ocp}$ variation with time curve for the NdFeB magnet in the pH modified 0.15 M $NaH_2PO_4$ solution.

The initial open circuit potential ($E_{ocp}$) of the NdFeB magnet is approximately −490 mV (SCE) and a steady state is obtained from the initial minutes of immersion until approxmiately 1 h. From 1.5–20 h, a steady logarithmic increase of the potential is seen. This period corresponds to growth of the more protective passive film. After 20 h, a plateau develops at a potential of approxmiately −270 mV (SCE). A similar $E_{ocp}$ against time curve was also found for pure aluminum in 0.5 N $Na_2SO_4$ solution for times above 200 min and ascribed to the growth of passive oxide film [20]. The potential increases until the passive film reaches its protective capacity resulting in stabilization of corrosion potential [21]. According to the literature, the film formed on Fe alloys in phosphate solution is believed to consist of iron phosphate ($FePO_4.2H_2O$) and iron oxide/hydroxide ($Fe_3O_4$-γ $Fe_2O_3$ and γ FeOOH) [22]. For the NdFeB magnets used, however, as the Nd rich phase is the most active phase, it is likely that $NdPO_4$ or a mixed Nd/Fe phosphate is also formed. The $E_{ocp}$ variation with time curve observed here, therefore is typical of passive metals in aerated solution and shows that the phosphating solution has an anodic passivating effect on the magnet for immersion times of approximately 1 day.

The porosity and inhomogeneities in the magnet can result in regions where the film does not fully cover the substrate. Hence, the potential measured may be a mixed potential having an intermediate value between the potential of passive areas and some slightly active anodic areas on the magnet. The phosphate solution has a dual role, to passivate the surface against corrosive attack and to repassivate regions where oxide film breakdown occurs. In general, localized attack occurs at defective areas in the surface oxide [23–25]. In the magnets used, pores may be preferential sites of attack; in particular where conditions give rise to crevice corrosion.

The results of electrochemical impedance spectroscopy (EIS) measurements at increasing times of immersion in 0.15 M $NaH_2PO_4$ acidified to pH 3.8 are shown in Fig. 3. The impedance significantly increases with time indicating that longer immersion times have a beneficial effect on the protective properties of the surface layer. Two time constants are observed for all immersion times, although for shorter times (2 h) the first constant at low frequencies is not so readily apparent. This suggests that as the time increases the two processes become increasingly separated due to an increasing difference in their kinetics. The constant at high frequencies is probably related to the porous nature of the magnet and that at low frequencies associated with faradaic processes. The phase angle at low frequencies increases with time, so this last process becomes more capacitive, i.e. there is increasing hinderance of the faradaic reactions.

The literature [26–28] reports that for porous electrodes, the EIS response at high frequencies depends on the a.c. signal penetrability in the pores. According to Song et al. [26], when the a.c. signal penetrates deeper than the pore's length, the electrode acts as a flat electrode. However, when the signal penetration is low, the response is only due to the pores and phase angles between 45 and 90° are obtained, depending on the length of the pore.

Fig. 4 shows a logarithmic increase of $|Z|_{10\ mHz}$ (modulus of impedance at 10 mHz), with time. The low frequency response, associated with faradaic processes here, suggests that as the phosphating time increases, the kinetics of the faradaic reactions slow down. This result supports the $E_{ocp}$ behavior with time, which we ascribe to growth of a passive oxide film. It is to be expected that passive film growth would increasingly block transport of species into pores in the magnet and consequently inhibit the faradaic processes.

Initial AES/EDX work has been performed to examine the composition of the phosphate film formed on different phases on the NdFeB magnet.

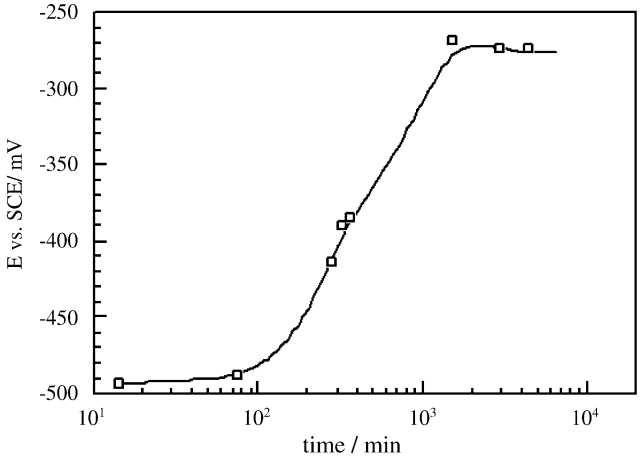


Fig. 2. Open circuit potential variation with time of NdFeB magnet in naturally aerated 0.15 M $NaH_2PO_4$ solution with the pH adjusted to 3.8.

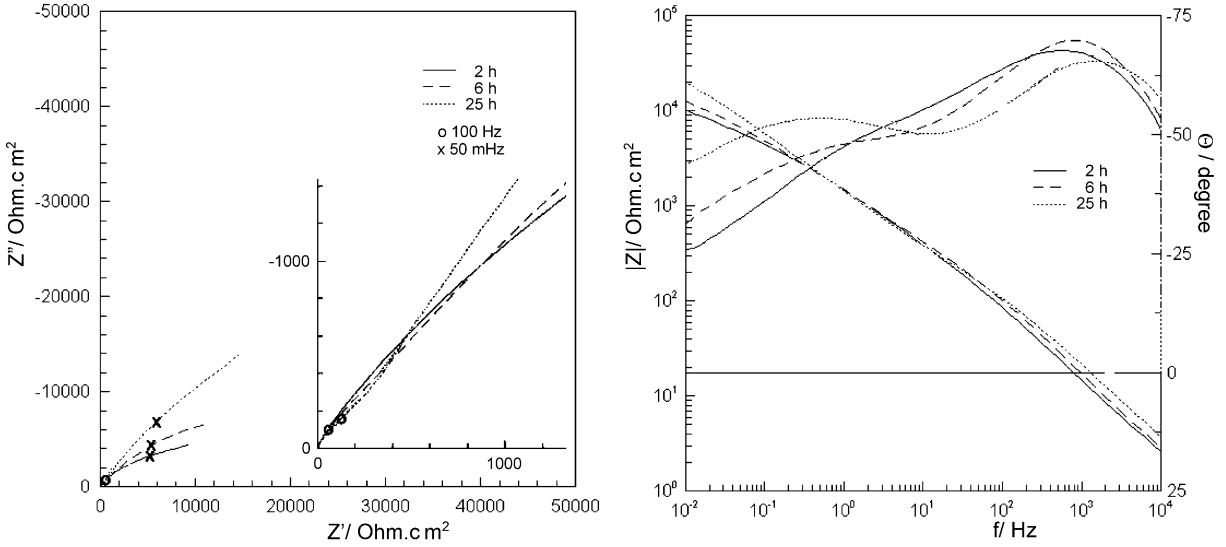


Fig. 3. Nyquist and Bode plots for NdFeB magnet at increasing times of immersion in 0.15 M $NaH_2PO_4$ solution with the pH adjusted to 3.8.

Fig. 5a,b present AES and EDX spectra from the phosphated magnet taken by rastering the electron beam over the Fe rich matrix phase of the alloy. The phosphate formed after a 24 h exposure to $NaH_2PO_4$ is sufficiently thick to show a strong P peak in the EDX spectrum. Fe, Nd, P and O are present in the AES spectrum in addition to C from overlayer hydrocarbon contamination. The presence of the strong Fe $L_3MM$ triplet between 570 and 700 eV and weak Nd $N_5M_{45}M_{45}$ and $N_{45}M_{45}N_{67}$ peaks at 733 eV and 840 eV, respectively, (see insert in Fig. 5b), indicate the phosphate to have a high Fe/Nd ratio. Auger and EDX point spectra acquired from the Nd rich phase are shown in Fig. 6a,b. In the EDX spectrum (Fig. 6b), a strong P peak is evident, showing that a phosphate coating has also formed on the Nd rich phase. In the AES spectrum, Fe, Nd, P, O, are again present but the Nd peaks are substantially stronger than those observed on the Fe rich phase. From the Auger spectra the Nd/Fe cationic ratio on the Nd rich phase is estimated to be approximately 4 times greater than on the Fe rich phase. The position of the P $KL_{23}L_{23}$ peak in spectra taken from the Fe rich phase was 1851 eV, typical of a phosphate and in good agreement with that obtained for iron phosphate at 1850.5 eV [29].

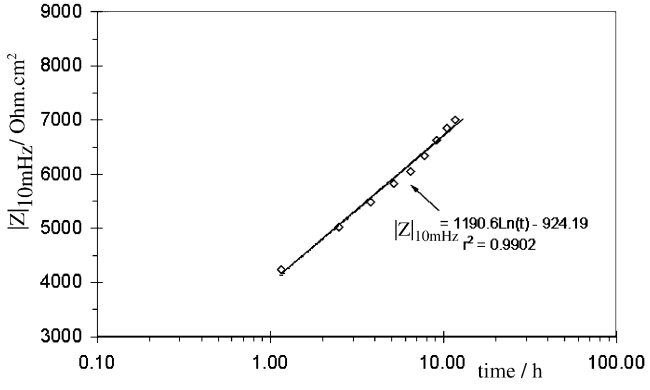


Fig. 4. Variation of of $|Z|_{10\ mHz}$ with phosphating time in 0.15 M $NaH_2PO_4$ solution (pH 3.8).

### 3.1. Corrosion test of phosphated magnets

Magnets phosphated for 4 h and 18 h were electrochemically tested in 0.01 mol $l^{-1}$ $Na_2SO_4$ solution and their corresponding EIS spectra are shown in Fig. 7.

The Nyquist diagrams of the phosphated magnets in 0.01 mol $l^{-1}$ $Na_2SO_4$ solution (Fig. 7) show flattened and incomplete capacitive arcs from high to medium frequencies, associated with the magnets phosphated for 4 h or 18 h, as indicated in the insert of this Figure. This arc is probably caused by charge transfer processes, which are affected by the presence of the phosphate layer. The increased impedances of the magnet phosphated for 18 h compared to that for 4 h show the beneficial effect of increasing phosphating time. At medium frequencies (100 Hz to 1 Hz) another flattened and incomplete arc is seen in the Nyquist diagrams associated with another time constant (also indicated by the peak in the Bode diagrams at this frequency range). This is followed at low frequencies by typical diffusion behavior (Warburg) possibly resulting from a gradual blockage of porosities in the magnet and the phosphate layer interfering with faradaic processes as the layer grows. The $|Z|_{10\ mHz}$ values for the phosphated (12 000 Ω $cm^2$) and unphosphated magnets (550 Ω $cm^2$) show an increase of nearly 22 times in the low frequency impedance due to phosphating.

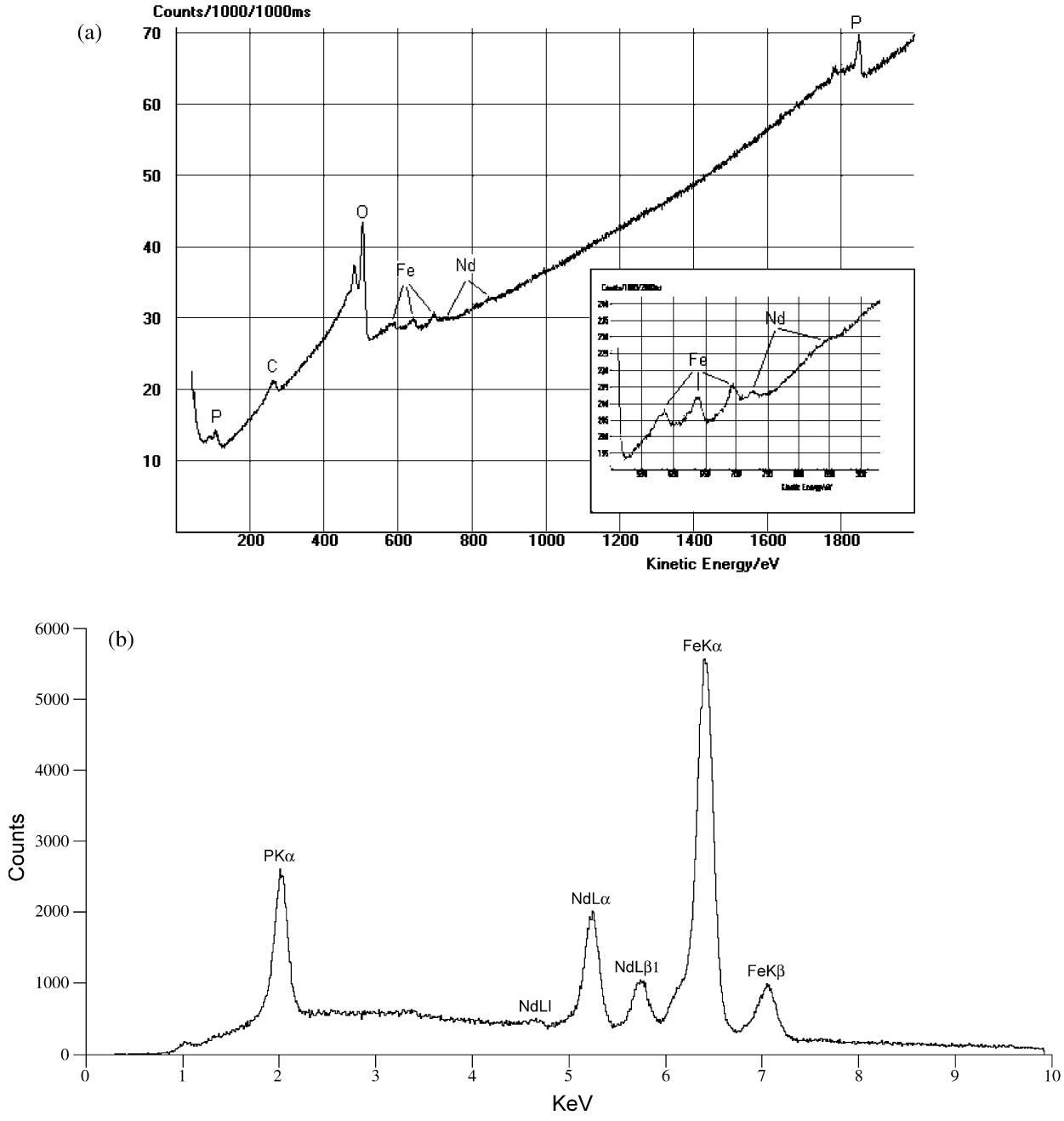


Fig. 5. (a) AES and (b) EDX spectra from the Fe rich ($\phi$ phase) for the phosphated magnet. Phosphating time: 24 h.

One of the applications of this kind of magnets is in dentistry such as retentive devices for overdentures and dental implants. A previous study showed localized corrosion associated with the magnet used in this investigation when immersed in a cell culture medium although its corrosion products presented no toxicity [30]. In Fig. 8, the EIS results of phosphated magnets in synthetic saliva are presented.

The Nyquist diagram for the unphosphated magnet shows a flattened and incomplete arc suggesting only one time constant whereas the corresponding Bode diagram indicates a large peak in the frequency range from $10^3$ Hz to 1 Hz, suggesting the interaction of two distinct processes. The Bode diagrams corresponding to phosphated magnets on the other hand, indicate two well separated distinct time constants. Increasing the phosphating time from 4 h to 18 h resulted in a large increase in the magnet impedance. The behavior at low frequencies was more capacitive and the corresponding peak shifted into lower frequencies as the phosphating time increased. This indicates slowing down of the faradaic reaction kinetics for longer phosphating times. The $|Z|_{10\ \mathrm{mHz}}$ values for unphosphated and 4h and

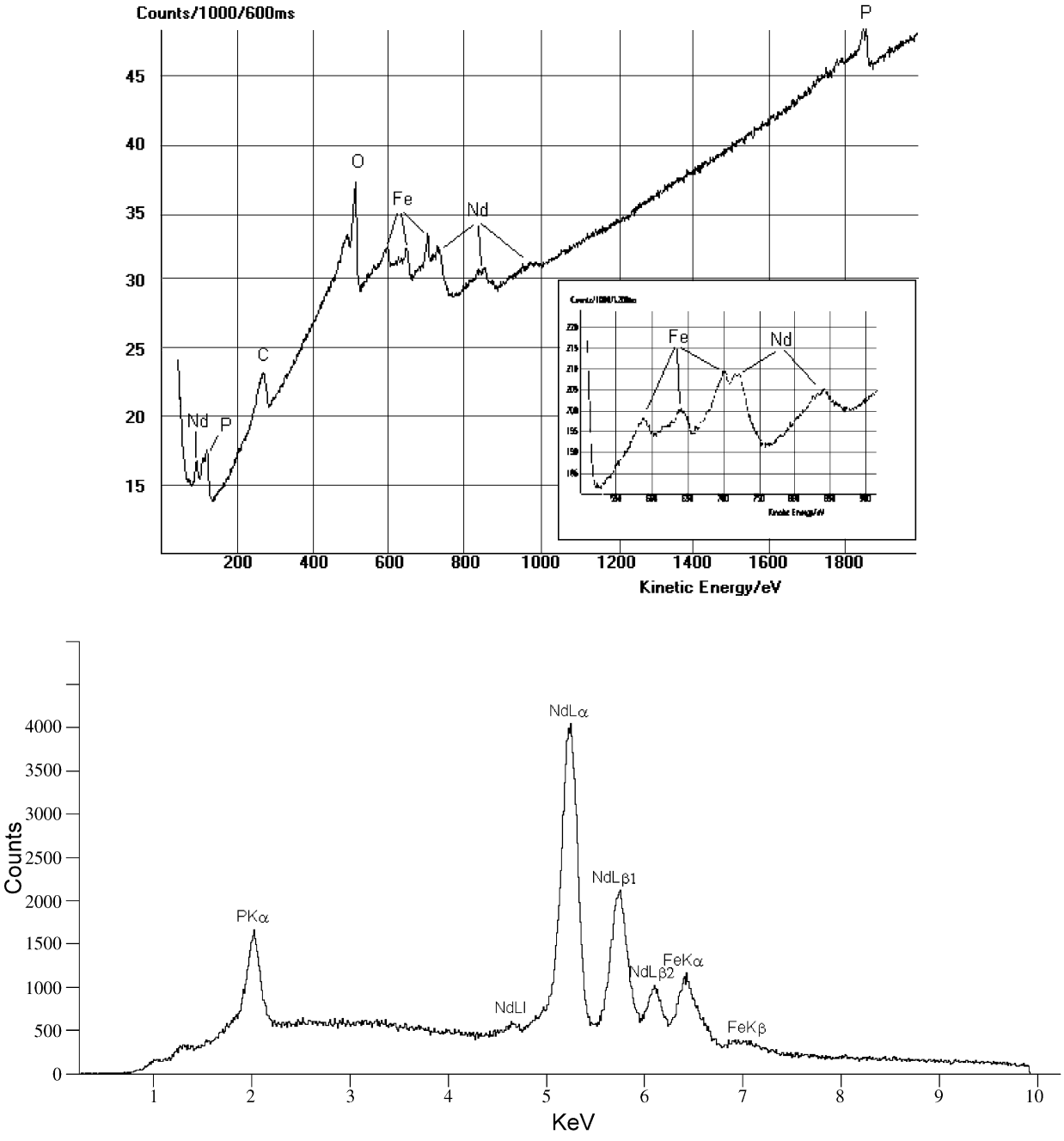


Fig. 6. (a) Auger and (b) EDX point spectra from the Nd rich phase for phosphated magnet. Phosphating time: 24 h.

18 h phosphated magnets were 6000 Ω $cm^2$, 18 000 Ohm $cm^2$, 70 000 Ω $cm^{2,}$ respectively.

The phosphate layer formed by immersion of the magnets in the 0.15 M $NaH_2PO_4$ solution acidified to pH 3.8 exhibited a bluish color. This film provided corrosion protection to the magnet during storage in enclosed sites such as the laboratory atmosphere. No visible signs of corrosion were seen on the surface after long periods of exposure (months) in the laboratory atmosphere whereas untreated specimens showed corrosion products on their surfaces after only a few days of exposure in the same atmosphere.

## 4. Conclusions

Immersion of sintered NdFeB magnets in 0.15 M $NaH_2PO_4$ solution acidified to pH 3.8 resulted in the deposition of a phosphate layer. Increasing the phosphating time from 4 h to 18 h had a beneficial effect on the character-

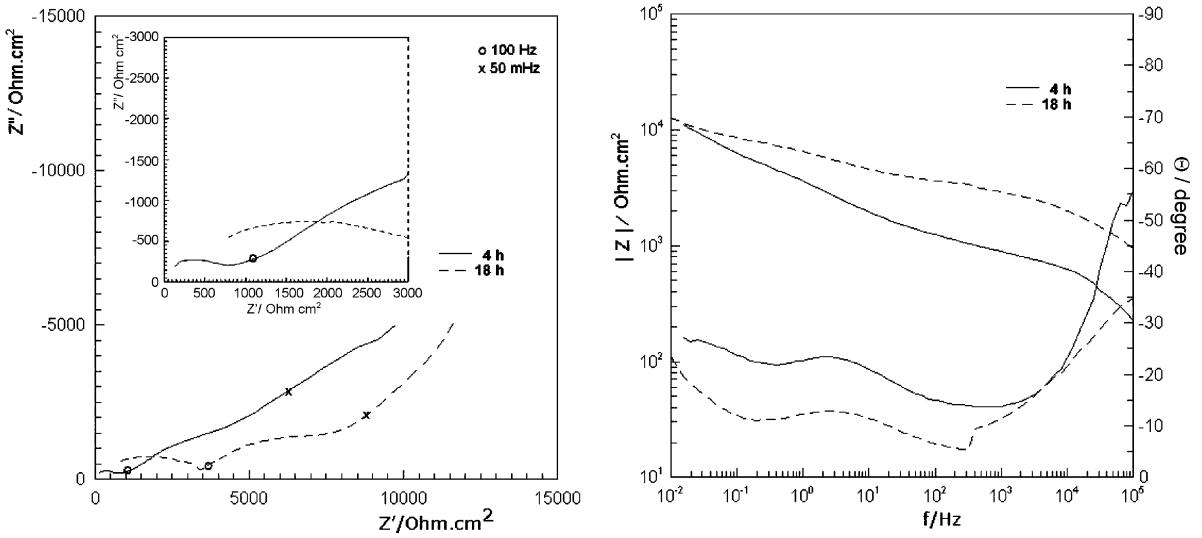


Fig. 7. EIS results of NdFeB magnets phosphated for 4 and 18 h 0.01 mol $l^{-1}$ $Na_2SO_4$ solution.

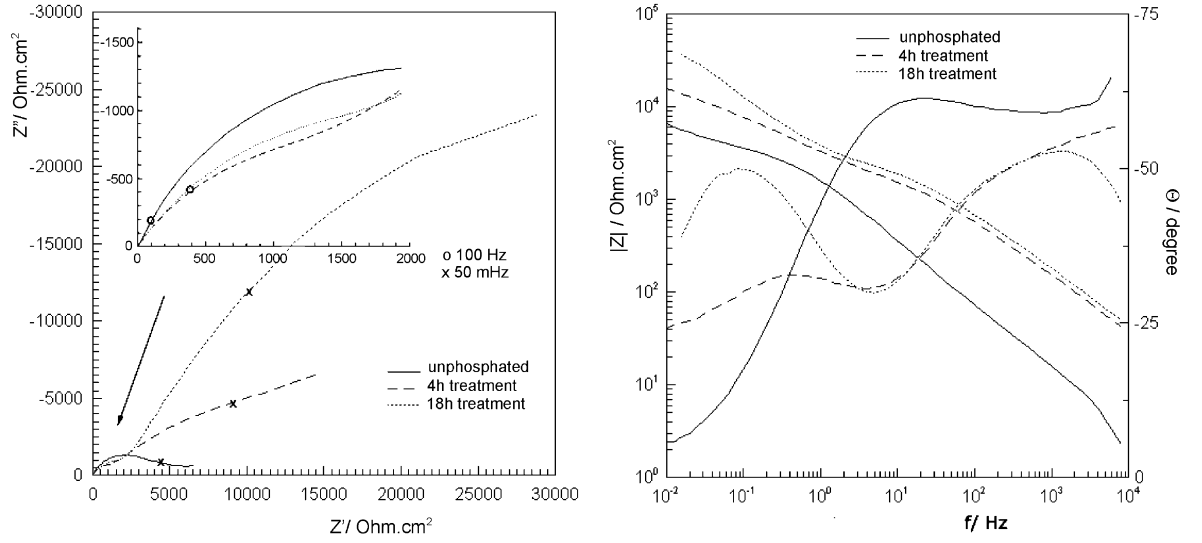


Fig. 8. Nyquist and Bode plots for magnets phosphated during 4 h and 18 h and then exposed in naturally aerated syntethic saliva solution.

istics of the phosphate film. AES/EDX results indicated phosphate formation on both Fe and Nd rich phases. The phosphate film caused a significant increase in the corrosion resistance of the magnet in mildly corrosive environments.

## Acknowledgments

The authors are grateful to FAPESP for financial assistance.

## References

[1] E.D. Dickens Jr, A.M. Mazany, J. Appl. Phys. 67 (1990) 4613.
[2] G.W. Warren, G. Gao, Q. Li, J. Appl. Phys. 70 (1991) 6609.
[3] S. Hirosawa, S. Mino, H. Tomizawa, J. Appl. Phys. 69 (1991) 5844.
[4] C.J. Willman, K.S.V.L. Narasimhan, J. Appl. Phys. 61 (1987) 3766.
[5] K. Tokuhara, S. Hirosawa, J. Appl. Phys. 69 (1991) 5521.
[6] H. Bala, G. Palowska, S. Szymura, V.V. Sergeev, Y.M. Rabinovich, J. Magn. Mater. 87 (1990) 1255.
[7] A.S. Kim, F.E. Camp, E.J. Dulis, IEEE Trans. Magn. 26 (1990) 1936.
[8] P. Tenaud, F. Vial, M. Sagawa, IEEE Trans. Magn. 26 (1990) 1930.
[9] J. Jacobson, A. Kim, J. Appl. Phys. 61 (1987) 3763.
[10] A.S. Kim, J. Appl. Phys. 64 (1991) 5571.
[11] B.E. Higgins, H. Oesterreicher, IEEE Trans. Magn. Magn. 23 (1987) 92.
[12] W. Bloch, K. Grendel, H. Staubach, in Proceedings 11th International Workshop on Rare Earth Magnets and Their Applications, Pittsburgh, Pa, 21–24 October 1990, p. 1081.
[13] T. Minowa, M. Yoshikawa, M. Honshima, IEEE Trans. Magn. Magn. 25 (1989) 3776.
[14] P. Mitchell, IEEE Trans. Magn. Magn. 26 (1990) 1933.
[15] T.S. Chin, R.T. Chang, W.T. Tsai, M.P. Hung, IEEE Trans. Magn. Magn. 24 (1988) 1927.

[16] I. Costa, I.J. Sayeg, R.N. Faria, IEEE Trans. Magn. Magn. 33 (1997) 3907.
[17] A.M. Saliba-Silva, I. Costa, K. Engineer. Mater. 189–191 (2001) 363.
[18] A.M Saliba-Silva, Ph.D. thesis, University of Sao Paulo, Brazil, 2001.
[19] A.M. Saliba-Silva, H.G. Melo, M.A. Baker, A.M. Brown, I. Costa, Mater. Sci. Forum 416–418 (2003) 54.
[20] M.S. El-Basiouny, A.A. Mazhar, Corrosion 38 (1982) 237.
[21] I. C. Lavos-Valereto, I. Costa, S. Wolynec, J. Biomed. Mater. Res. 63 (2002) 664.
[22] M. Cohen, Corrosion 32 (12) (1976) 461.
[23] L.G. Gainer, G. R. Wallwork, Corrosion 35 (1979) 435.
[24] M.A. Baker, J.E. Castle, Corros. Sci. 33 (1992) 1295.
[25] M.A. Baker, J.E. Castle, Corros. Sci. 34 (1993) 667.
[26] H.-K. Song, Y.-H. Jung, K.-H. Lee, L.H. Dao, Eletrochim. Acta 44 (1999) 3513.
[27] H.-K. Song, H.-Y. Hwang, K.-H. Lee, L.H. Dao, Eletrochim. Acta 45 (2000) 2241.
[28] I.V. Aoki, M.C. Benard, S.I. Cordoba de Torresi, C. Deslouis, H.G. de Melo, S. Joiret, et al., Eletrochim. Acta 46 (2001) 1871.
[29] R. Franke, Th. Chasse, P. Streubel, A. Meisel, J. Electron Spectrosc. Relat. Phenom. 56 (1991) 381.
[30] S.O. Rogero, M. Saiki, E.S.K. Dantas, M.C.L. Oliveira, A S. Cruz, T.I. Ikeda, et al., Mat. Sci. Forum 416–418 (2003) 76.